Available online at www.sciencedirect.com
ScienceDirect
Applied Catalysis B: Environmental 81 (2008) 1–13
APPLIED CATALYSIS B: ENVIRONMENTAL
www.elsevier.com/locate/apcatb

Zinc-aluminates for an in situ sulfur reduction in cracked gasoline

R. Quintana-Solórzano *, J.S. Valente, F.J. Hernández-Beltrán, C.O. Castillo-Araiza

Instituto Mexicano del Petróleo, Eje Central Lázaro Cárdenas Norte 152 C.P., 07730 México, D.F., Mexico

Received 12 September 2007; received in revised form 21 November 2007; accepted 6 December 2007
Available online 15 December 2007

Abstract

Using additives remains as an attractive alternative for an in situ sulfur reduction in cracked gasoline since it is a practical, flexible and economical option. Zinc-aluminates prepared by the sol–gel method are used as additives for reducing sulfur in gasoline from the cracking of a high-sulfur feed in a fixed-bed bench reactor. Products distribution and feed conversion are not dramatically altered after incorporating the additive to the base catalyst with some effect on gasoline and its octane number and coke. A decrease in the gasoline sulfur content of up to 35 wt% including benzothiophene, and up to 50% excluding benzothiophene, is observed when blending the zinc-aluminates to the base catalyst, which is caused by lowering the C_1 to C_4 alkyl-thiophenes content. The zinc content of the zinc-aluminates has a positive effect on the gasoline sulfur reduction. It is suggested that together with the direct cracking of adsorbed thiophenic species on the additive, a further gasoline sulfur decrease is possible through cracking of saturated thiophenic species formed by hydrogenation of adsorbed thiophenic species with hydrogen produced in situ in the additive. The obtained results also demonstrate that solids with higher Lewis acidity are not unfailingly the most effective for gasoline sulfur reduction.

Keywords: Catalytic cracking; Gasoline sulfur reduction; Zinc; Zinc-aluminates; Additive

1. Introduction

Fluid Catalytic Cracking (FCC), a process that converts heavy crude oil fractions with a distillation range above 623 K at temperatures of around 800 K in the presence of a Y-zeolite-based catalyst, continues being a key part of the modern refining scheme [1]. It leads to a very large volume of automotive fuels, i.e., gasoline and diesel, and petrochemicals, i.e., ethylene and light olefins. More than 35 vol% of the gasoline consumed around the world is supplied by the FCC process [2]. However, the cracked gasoline is also, by far, the most important contributor to the sulfur in the gasoline pool with levels close to 90 wt% [3].

Nowadays, environmental regulations for fuels specifications and atmospheric emissions are evolving to more severe limits, which are clearly in an opposite direction with respect to the quality of the worldwide processed crude oils, e.g., higher content of sulfur, nitrogen and metals. For the gasoline, for instance, US EPA has recommended a reduction to 30 ppm of sulfur to 2008 whereas in the European Union this value is to be set below 50 ppm [4,5].

Although the proportion of sulfur feed that ends up in the gasoline fraction after cracking is, strictly speaking, catalyst and feedstock dependent [6,7], higher sulfur levels in the feed typically leads to higher gasoline sulfur content. Sulfur in gasoline affects negatively the performance of automobile catalytic converters and, after combustion, produces SO_x, an important atmospheric oxidant and a precursor of the unwanted acid rain [8].

Decreasing the sulfur content in the cracked gasoline is crucial for lowering the gasoline pool sulfur. Several alternatives exhibiting advantages and disadvantages are currently available for lowering the sulfur levels in the cracked gasoline, viz., feed and gasoline hydrotreating, gasoline sulfur adsorption and gasoline hydrofinishing [9]. Hydrotreating is an effective option, notwithstanding, apart from requiring high invest costs for the installation of those process and high hydrogen volume, it is traditionally accompanied by a gasoline octane decrease. The latter effect is also observed for the case of hydrofinishing [10]. Recently, however, hydrodesulfurization processes, for instance, the Prime D and the Prime G+ by IFP/Axens, have reported a deep sulfur reduction with a low penalty

* Corresponding author. Tel.: +52 55 9175 8516.
E-mail address: rquintana@imp.mx (R. Quintana-Solórzano).

0926-3373/$ – see front matter © 2007 Elsevier B.V. All rights reserved.
doi:10.1016/j.apcatb.2007.12.001

in the gasoline octane number [11]. Thus, very attractive results a combination of these processes with an in situ gasoline sulfur reduction. This can relief the feed for the hydrodesulfurization processes which ultimately may improve their sulfur reduction margins.

As an alternative for an in situ gasoline sulfur reduction in FCC, catalysts have been reformulated to increase their hydrogen transfer activity resulting in sulfur reducing levels below 25 wt% with a detrimental effect on gasoline octane and LPG olefinicity, however [12]. A second option for an in situ gasoline sulfur reduction is the use of special additives typically consisting of a metal oxide, e.g., zinc, zirconium, manganese, cobalt, etc., on an alumina or titania support that have reported reduction levels in the range 20–40% when added to the reactor bed [12,13]. The latter option is very promising taking into consideration the compromise between effectiveness and cost. Increasing the efficiency of these additives is a challenge considering the refractoriness to cracking of the thiophenic species contained in the cracked gasoline fraction [14,15].

Several studies dealing with the use of additives for an in situ gasoline sulfur reduction are available in literature [16–20], only some of them, however, under attractive conditions for industrial practice. The effectiveness of the gasoline sulfur reducing additives has been associated to their acidity, in particular Lewis sites, due to the basic nature of the cracked gasoline sulfur compounds [13,19,21]. The Lewis nature of the acid sites of these additives, however, has been reported to increase coke formation [6,19].

In this work, the potential of a set of zinc-aluminates prepared by sol–gel with a different zinc content to reduce the sulfur in the cracked gasoline is investigated. A high-sulfur synthetic mixture of gas oil streams coming from a Mexican Maya crude oil has been subjected to catalytic cracking in a fixed-bed bench scale reactor at operating conditions relevant for the industrial practice. Attention is also paid on the effect of the zinc-aluminates addition to a base catalyst on the cracked products distribution and on the quality of the cracked gasoline.

2. Experimental and procedures

2.1. Materials

2.1.1. Zinc-aluminates synthesis

Three zinc-aluminates denoted as SG12Zn, SG17Zn and SG22Zn, the number corresponding to the nominal zinc content, were prepared by the so-called sol–gel method.

Tri-*sec*-butoxide of aluminum (TBA) from Aldrich with 97% of purity was used as aluminum precursor while ethanol (EtOH) 99.5% of purity from J.T. Baker was employed as solvent. Nitric acid (Baker, 70%) was used as hydrolysis catalyst and zinc nitrate (Aldrich, 99.99%) was the zinc source.

The molar ratios of reactants were TBA:EtOH = 1:60, TBA:HNO_3 = 1:0.03, Zn:EtOH = 1:60, and TBA:H_2O = 1:1. To prepare 10 g of sample SG22Zn, for instance, the following amount of reagents is required, viz., 536 ml of EtOH, 40 ml of TBA, 1.53 ml of HNO_3, 10.03 g of $Zn(NO_3)_2{\cdot}2H_2O$ dissolved in 117.8 ml of EtOH and 0.03 ml of H_2O.

TBA was dissolved in ethanol and then refluxed at 348 K. The resulting mixture was stirred for 1 h. A 3N HNO_3 solution was added drop-wise to this mixture under vigorous stirring for 1 h resulting in a transparent solution. The latter was cooled down at room temperature. The corresponding amount of zinc nitrate was dissolved in ethanol and then added to the solution under vigorous stirring for 2 h. Deionized water was slowly added, allowing the hydrolysis to complete itself. The formed gel was poured into a glass vessel, aged for 24 h at room temperature and dried overnight at 373 K. Afterwards, the zinc-aluminates were calcined at 973 K for 4 h in static air atmosphere.

2.1.2. Characterization of the zinc-aluminates

The chemical composition of the zinc-aluminates was determined by Inductively Coupled Plasma Atomic Emission Spectrometry (ICP-AES) in a PerkinElmer Mod OPTIMA 3200 Dual Vision.

The X-ray powder diffraction patterns of fresh and calcined samples packed in a glass holder were recorded at room temperature with Cu Kα radiation in a Bruker Advance D-8 diffractometer having a θ–θ configuration and a graphite secondary-beam monochromator. Diffraction intensity was measured between 10° and 110°, with a 2θ step of 0.02° for 8 s per point.

Textural properties of calcined samples were analyzed by N_2 adsorption–desorption at 77 K on an AUTOSORB-I apparatus. Prior to the analysis, the samples were outgassed in a vacuum (10^{-5} Torr) at 673 K for 5 h. The total specific surface area was calculated by using the Brunauer–Emmett–Teller (BET) method, and the pore size distribution and total pore volume were determined by the Brunauer–Joyner–Hallenda (BJH) method.

Pyridine (Py) adsorption in a Fourier Transform Infrared (FTIR) spectrometer Nicolet model 170-SX was performed on calcined samples in order to determine nature, quantity and strength of acid sites. FTIR-Py spectra were recorded on self-supported wafers which were activated by outgassing in a pyrex cell, with CaF_2 windows at 673 K under vacuum at 1×10^{-6} Torr. After this pretreatment, samples were exposed for 20 min to pyridine by breaking the capillary tube containing 100 μl of this substance. After adsorption, the infrared spectrum was recorded with the sample temperature fixed from room temperature to 773 K.

2.1.3. Reference additive

A commercial additive for reducing sulfur in cracked gasoline denoted as red-S was used as reference for comparing the catalytic performance of the tested zinc-aluminates. According to the manufacturer, it is composed of zinc oxide supported on alumina.

2.1.4. Reference catalyst

To evaluate the catalytic performance of the synthesized zinc-aluminates as well as the commercial additives, they were blended with a commercial equilibrium catalyst, denoted as ref Ecat, obtained from a refinery in Mexico. Using an equilibrium

Table 1
Physical and chemical properties of the reference equilibrium catalyst (ref Ecat) employed during the catalytic cracking experiments

Property	Value
Alumina (wt%)	31.9
Rare earths (wt%)	1.22
Total specific surface area (m^2/g)	160
Zeolite specific surface area (m^2/g)	119
Zeolite to matrix specific surface area ratio	2.9
Pore volume (m^3/kg)	131×10^{-6}
Average bulk density (kg/$m^{3)}$	910
Unit size cell (nm)	2.424
Vanadium (ppm)	2500
Nickel (ppm)	379
Sodium (ppm)	2648
Iron (ppm)	5166

catalyst is more realistic than a metals-free steam deactivated catalyst since a possible effect of the metals, which are invariantly present in an Ecat, on sulfur reduction is accounted for [6].

The most significant chemical and physical properties of the ref Ecat are presented in Table 1. The active component of the ref Ecat is a REUSY, i.e., a rare earth exchanged ultra-stable Y zeolite. The combination of the USY zeolite with rare earths in a FCC catalyst is typical of a so-called barrel-octane gasoline catalyst. The zeolite contributes to practically 75% of the total specific surface area of this catalyst. The level of contamination with metals, in particular nickel and vanadium, is moderated according to typical values reported in the literature of about 600 ppm for nickel and 2000 ppm for vanadium [22].

2.2. Feed

For the cracking experiments, a synthetic feed has been prepared by blending three hydrocarbons streams from a Mexican Maya crude, viz., 38 vol% of atmospheric heavy gas oil, 18 vol% of light vacuum gas oil and 44 vol% of heavy vacuum gas oil. According to the average properties reported in Table 2, this is a feed with a sulfur level above 2.5 wt% which is characteristic of a high-sulfur feed. In addition, this feed is also characterized by containing a relatively high proportion of naphthenic and aromatic hydrocarbons as well as metals in comparison with feeds not derived from a Maya crude oil as was pointed out elsewhere [6]. The relatively high content of naphthenes may enhance the relative rate of hydrogen transfer based on the hydride donor capacity of this type of hydrocarbons which ultimately may promote the coke formation [12]. Such properties make this feed particularly attractive for performing in situ sulfur reduction studies.

2.3. Reaction conditions and products analysis

The catalytic performance of the ref Ecat and the ref Ecat/additive blends was studied in an AUTOMAT set-up by Xytel Corp equipped with a conventional fixed-bed Micro-Activity Test (MAT) reactor. Details about the reactor configuration are given in the ASTM-D-3907 method. Prior to load the ref Ecat and the additives to the reactor, they were sieved to a particle size range between 60 and 200 μm in order to have a homogeneous bed, to filter out high pressure drops in the reactor and to eliminate preferential flows and channeling in the bed. The ref Ecat was further calcined for 4 h using an air static atmosphere at 853 K to eliminate any residual coke which may have an effect on the cracking results.

Table 2
Properties of the feed used for the catalytic cracking experiments

Property	Value
Specific gravity (298/277 K)	0.9052
Distillation ASTM-D-1160	
IBP (K)	496
5/10/30 vol% (K)	516/526/580
50/70/90 vol% (K)	682/748/788
FBP (K)	821
Molecular weight (g/gmol)	290
Conradson carbon (wt%)	0.23
Aniline temperature (K)	342
Refraction index 0/20	1.5055
K factor (UOP)	11.55
Fe/Cu/Na/V/Ni (ppm)	0.13/0.02/<0.02/1.08/0.07
Sulfur (wt%)	2.69
Total nitrogen (ppm)	1498
Carbon in aromatics (wt%)	22.2
Carbon in naphthenes (wt%)	20.9
Carbon in paraffins (wt%)	56.9

A cracking run consisted of a set of four experiments, each of them at a given catalyst to oil ratio (C/O). An initial run on the ref Ecat was done to determine its performance in the absence of any additive. All other cracking runs were carried out on ref Ecat/additive blends. The reactor bed mass amounted to 4.0 g for all the runs. When evaluating ref Ecat/additive blends, the reactor bed consisted of 3.6 g of the former and 0.4 g of the latter, which is equivalent to 10 wt% of additive in the blend.

The reactor was operated in the isothermal mode at 793 K. This temperature falls in the range of typical riser outlet temperatures of commercial FCC units. The feed was preheated at 373 K and injected to a constant inlet flow rate equal to 0.017 g/s. The feed injection time was spanned from 37 to 75 s in order to vary the catalyst to oil ratio which, in turn, ranged from 3 to 6 g/g. Having a C/O range is necessary to be able to assess the evolution of the cracked products on a constant feed conversion basis, as has been recommended by others [23,24].

A cracking experiment consists of three stages, i.e., feed injection/cracking, catalyst stripping and spent catalyst regeneration. The injected feed, admixed with nitrogen as diluent, is vaporized while flowing down to the reactor and cracks when contacts the catalyst bed. Once the reaction is over, the catalyst bed is subjected to stripping with nitrogen flow during 600 s for exhausting residual occluded hydrocarbons. The nitrogen/stripped hydrocarbons stream is added to the gaseous cracked products and then the mixture is quantified in a glass bottle by water displacement at atmospheric pressure and room temperature. The liquid product formed during the cracking reactions is collected in a glass receiver cooled at 273 K. The coke deposited on the stripped spent catalyst is

burnt up under with air at 923 K. The amount of coke is indirectly measured by quantifying the CO_2 formed during the catalyst regeneration in a Horiba Mod VIA-500 IR analyzer. After burning out the coke, the catalyst or catalyst/additive blends were used for the next run.

The gaseous products composed of hydrogen, C_1 to C_4 hydrocarbons and a small amount of non-condensed gasoline, mainly C_5–C_6, were analyzed by chromatography in a HP-6890 GC equipped with FID and TCD detectors and a set of columns using a Separation Systems application. The liquid product referred as to syncrude composed of gasoline, light cyclic oil (LCO) and heavy cyclic oil (HCO) was analyzed in a HP-6890 GC with a FID detector using a 10 m/0.53 mm/2.63 μm megabore BPX-1 methyl-silicone column, in accordance with ASTM-D-2887 method for a simulated distillation. Mass recovery ranged between 97 and 102 wt%.

A detailed hydrocarbon analysis also referred to as a PONA analysis was performed for the gasoline fraction in a HP-6890 GC equipped with a DB-Petro 100 m/0.251 mm/0.5 μm capillary column and split injector. Chromatographic octane numbers, GC-RON (research octane number) and GC-MON (motor octane number), were computed based on the octane number of the individual species identified and their amount.

A Sievers Mod 355 chemiluminiscence detector coupled to the simulated distillation GC was used for the sulfur analysis of the syncrude. The sample vapors exiting the FID of the GC are burned with air and hydrogen at 1073 K. The combustion gases are then sucked into a chamber where the corresponding sulfur compounds react with an excess of ozone via a chemiluminiscent reaction that produces light which is detected by a photomultiplier tube. The total sulfur in the syncrude and the sulfur content in its different cuts, i.e., gasoline, LCO and HCO, were obtained. By injecting pure compounds, the most salient sulfur species in cracked gasoline such as thiophene, C_1–C_4 alkylthiophenes and benzothiophene were identified and then quantified.

2.4. Calculations

In refinery terms and in line with the ASTM-D-5154 method, cracked products are typically classified according to their boiling point and carbon number in the following cuts, viz., dry gas: H_2 and C_1–C_2; LPG: C_3–C_4; gasoline: 221–494 K; LCO: 494–616 K, and HCO: 616 K+. The coke deposited on the catalyst completes the mass balance. The yield of a cut i is calculated by:

$$\text{yield}_i = \frac{\text{mass formed of cut } i}{\text{total feed mass}} 100 \quad (1)$$

Assuming that the feed is composed of LCO and HCO, the feed conversion is defined in terms of the mass of gas oil converted to dry gas, LPG, gasoline and coke. This can be expressed by:

$$\%\text{feed conversion} = 100 - \text{yield}_{\text{HCO}} - \text{yield}_{\text{LCO}} \quad (2)$$

Notice that in the MAT test, conversion and products yield correspond to average values since the cracked products formed during the reaction period are collected, quantified and analyzed afterwards.

By analogy with Eq. (1), the sulfur distribution to the various cuts can also be expressed in terms of the mass of the sulfur in the feed, i.e., sulfur yields. This is calculated for a cut i as follows:

$$\%\text{sulfur feed to cut}_i = \frac{\text{sulfur mass ended up in cut } i}{\text{total sulfur feed mass}} 100 \quad (3)$$

Also by analogy with Eq. (2), the conversion of the sulfur contained in the feed can be calculated by:

$$\%\text{sulfur feed conversion} = 100 - \text{sulfur feed in HCO} - \text{sulfur feed in LCO} \quad (4)$$

By using Eq. (3) for the analysis of the sulfur in gasoline, it is possible to filter out differences in gasoline yields when comparing the sulfur content in concentration terms.

3. Results and discussion

3.1. Additives characterization

3.1.1. Chemical composition and structural properties

ICP-AES analysis shows a very good agreement between nominal and real amount of zinc, as is presented in Table 3. Hence, the zinc content for the samples SG12Zn, SG17Zn and SG22Zn was 12, 17 and 22 wt% respectively; whilst that of the additive red-S was 11 wt%.

In the X-ray diffraction patterns displayed in Fig. 1, it is observed that the pristine zinc-aluminates are amorphous, which has also been observed elsewhere [25,26] on alumina-based materials out of the sol–gel method. The X-ray diffraction patterns of the sample red-S in the fresh and in the calcined form are practically the same which indicates that the additive had already been subject to calcination by the manufacturer.

After calcination at 973 K for 4 h, the presence of poorly crystallized γ-alumina and crystalline $ZnAl_2O_4$ spinel is observed in the zinc-aluminates as is depicted in Fig. 1. Relative differences in γ-alumina and $ZnAl_2O_4$ spinel phases

Table 3
Physical and chemical properties of zinc-aluminates and commercial additives used during the catalytic cracking experiments

Sample	Zinc content (wt%)	Total specific surface area (m^2/g)	Pore volume (cm^3/g)	Average pore diameter (nm)
SG12Zn	12	211	0.39	7.5
SG17Zn	17	163	0.32	8.0
SG22Zn	22	146	0.31	8.7
red-S	11	151	0.34	6.4

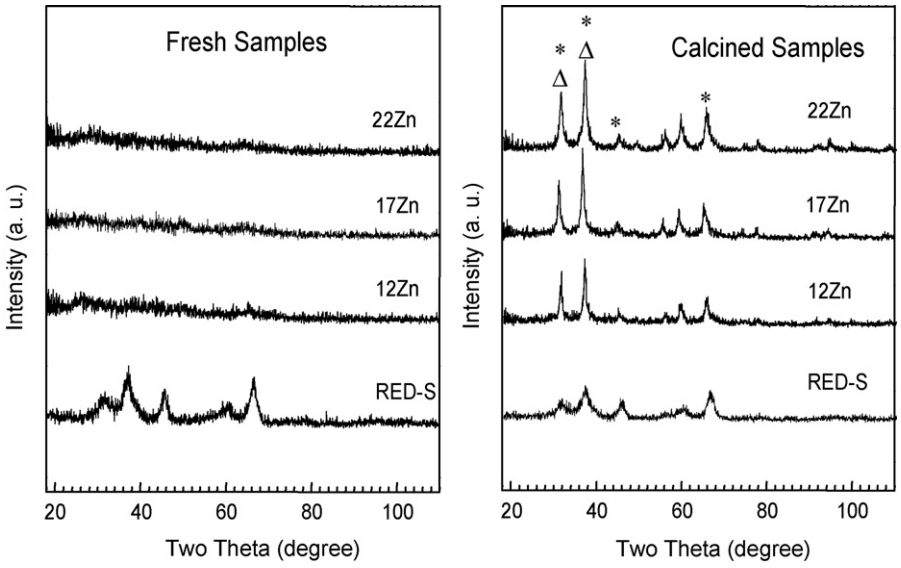

Fig. 1. X-ray spectra of the zinc-aluminates and the reference additive red-S before and after calcination under air atmosphere at 973 K for 4 h: (*) γ-alumina and (Δ) $ZnAl_2O_4$.

are observed for the zinc-aluminates, namely $ZnAl_2O_4$ spinel phase increases proportionally with the zinc content while the crystallinity of the γ-alumina does not change even after undergoing the same thermal treatment. For instance, it is likely that for the SG12Zn sample, the $ZnAl_2O_4$ spinel phase is highly dispersed on a γ-alumina matrix. Finally, based on the peak width it can be inferred that the zinc-aluminates have a larger crystal size in comparison with the additive red-S.

3.1.2. Textural properties

From Table 3, the total specific surface area of the zinc-aluminates is in the range 146–211 m^2/g, the pore volume from 0.31 to 0.39 cm^3/g and the average pore diameter from 7.5 to 8.7 nm. It is clear that the total specific surface area and the average pore volume decrease with the zinc content. According to the X-ray patterns in Fig. 1, a $ZnAl_2O_4$ spinel phase that increases with the zinc content is formed after calcination at 973 K for 4 h. It is reported in literature [27] that $ZnAl_2O_4$ spinel exhibits a lower total specific surface area compared with γ-alumina but with a remarkable higher thermal stability and mechanical resistance. A further decrease in the total specific surface area of the zinc-aluminates by a γ-alumina pore blockage by $ZnAl_2O_4$ might occur albeit to a lesser extent because of the relatively low variation of the pore volume and the pore diameter with the zinc content.

A comparison of the textural properties of the reference additive red-S with the sample SG12Zn which have a similar zinc content, shows that the latter has a higher total specific surface area and pore volume, which indicates that solids by the sol–gel method displays higher surface area than those obtained by traditional ones [25,26]. The control of textural properties with additives is of a paramount importance for enhancing the access of bulky hydrocarbons to active sites. In fact, there is an increase in the average pore size diameter with the zinc content whereas the reference additive red-S showed the lowest pore size diameter based on the information in Table 3.

3.1.3. FTIR pyridine adsorption

The adsorbed pyridine on calcined zinc-aluminates and the additive red-S displayed absorption bands at 1580, 1490 and 1446 cm^{-1}, see spectrum of Fig. 2 for sample SG17Zn, which correspond to pyridine adsorbed on Lewis acid sites [28]. Needless to say that the band at 1490 cm^{-1} corresponds, strictly speaking, to both Lewis and Brönsted acid sites. However, considering that a band at 1540 cm^{-1} attributed to Brönsted acid sites does not appear in the spectra and taking into consideration the nature of the zinc-aluminates, it is deduced that the observed band at 1490 cm^{-1} indicates only the presence of Lewis sites. Table 4 summarizes the FTIR-Py

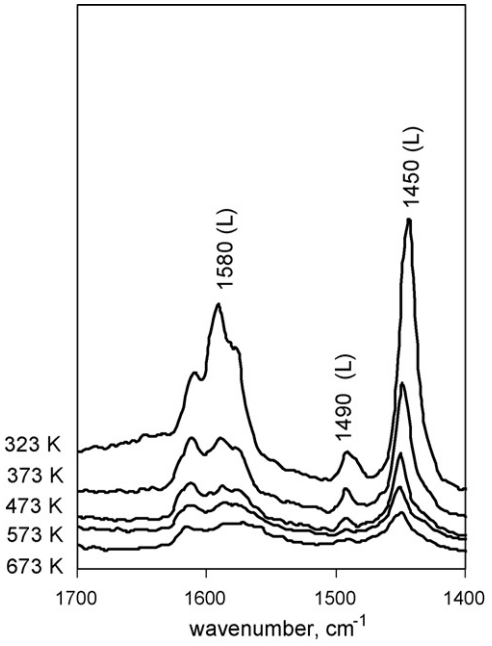

Fig. 2. FTIR-Py spectra of pyridine adsorbed from 50 to 673 K on sample SG17Zn.

Table 4
Amount of pyridine adsorbed on calcined zinc-aluminates and the ref Ecat as a function of the desorption temperature and corresponding calculated intrinsic acidity

Temperature (K)	Acidity (μmol/g)				
	SG12Zn	SG17Zn	SG22Zn	red-S	ref Ecat
323	744	643	357	613	147
373	343	278	157	293	44
473	182	149	66	191	22
573	130	97	6	105	10
673	87	68	0	70	0
773	0	0	0	0	0
IA[a] (μmol/m^2)	3.53	3.94	2.44	4.06	0.92

[a] IA: Intrinsic acidity corresponding to the amount of pyridine adsorbed at 323 K per total specific surface area.

quantitative results for all the additives and the ref Ecat. The latter has both Brönsted and Lewis acid sites, the former sites associated to its zeolitic component [13].

From the total amount of pyridine adsorbed on the solids and based on the fact that stronger acid sites are associated to pyridine retained at higher temperatures, the total Lewis acidity and their strength decrease with the zinc content. For instance, SG12Zn sample exhibited the highest value, 774 μmol/g, whereas the SG22Zn the lowest one, 357 μmol/g. Concerning the acid strength, there is still pyridine retained on SG12Zn, SG17Zn and red-S at 673 K which is not the case on SG22Zn.

To investigate further on the acid properties of the zinc-aluminates, the intrinsic acidity (IA), corresponding to the total amount of pyridine adsorbed per square meter of total specific surface area, was calculated. In Table 4 one can see that the sample SG17Zn exhibited the highest IA value, i.e., 3.9 μmol/m^2, within the zinc-aluminates series, whereas SG22Zn the lowest one, 2.4 μmol/m^2. The reference additive, red-S displayed an IA equal to 4 μmol/m^2 which is very close to that observed for SG17Zn. In aluminas, it has been pointed out that their Lewis acidity is related to tetrahedral aluminum coordination and to the chemical nature of its neighbors [29].

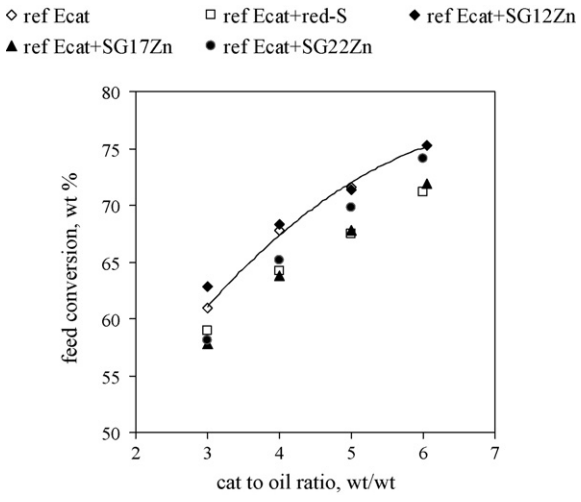

Fig. 3. Feed conversion as a function of the catalyst to oil ratio. The solid line is a trend line drawn for the ref Ecat experimental data.

The creation of aluminum coordinately unsaturated sites (Al-CUS), which is accompanied by a redistribution of the charge on the aluminum and oxygen atoms, plays a key role for controlling the acidity of an intended alumina-based catalyst [30].

For the zinc-aluminates, the information contained in Table 4 indicates that Lewis acidity decreases with the zinc content, which can be explained by the fact that zinc produces a $ZnAl_2O_4$ spinel phase with alumina cations, as was detected by the XRD technique. Thus, assuming that this normal spinel structure is formed, Zn^{2+} occupies the tetrahedral sites while Al^{3+} the octahedral ones [31]. For each zinc atom in the spinel structure, two aluminum atoms in octahedral coordination are required, thereafter, the Al-CUS decrease with the zinc content which justifies the Lewis acidity trend observed for the zinc-aluminates.

3.2. Additives cracking performance

3.2.1. Cracking activity

Determining the effect of incorporating additives to the main catalyst on feed conversion (and coke formation, cfr. infra) is important to define whether the catalyst circulation and, hence, the thermal balance, will be modified with respect to a base circulation in a commercial unit.

For our experiments, all samples of additives added to the reference Ecat except for SG12Zn, exhibited a slight decrease in feed conversion at a given C/O, as is illustrated in Fig. 3, which is in agreement with information reported in literature [10,32]. More specifically, for the studied C/O range a decrease between about 3 and 6 wt% units of conversion was observed for the ref Ecat/additive blends investigated. This indicates, in general, a lower cracking capacity of the additives compared with the ref Ecat since a fraction of the latter has been replaced to incorporate the corresponding additive. The fact that the addition of the SG12Zn did not lead to feed conversion decrease appears to be associated, in principle, to its higher total specific surface area and larger pore volume together with its higher Lewis acidity, compared with the other two zinc-aluminates. In other words, it can be assumed that the γ-alumina, present in a higher proportion on the sample SG12Zn due to its lower zinc ($ZnAl_2O_4$) content, is providing some additional catalytic activity to this additive. The use of alumina-based additives for bottoms upgrading in FCC has been reported elsewhere [33]. However, the fact that the sample SG22Zn displayed a higher activity compared with SG17Zn, in particular at high C/O, indicates a higher acidity or higher total specific surface area does not lead invariably to higher feed conversions. It is evident that apart from the textural and acid properties of the zinc-aluminates there are some process issues entering to the scene. In fact, it is observed in Fig. 3 that the relative differences in cracking activity of the zinc-aluminates are C/O dependent. The γ-alumina in the zinc-aluminates can provide some catalytic activity, but based on their acid properties zinc-aluminates may also work as a fed coke precursors trap, due to the basic character of the latter. The C/O determines the amount of coke deposited on the catalyst, in short, a lower C/O results in

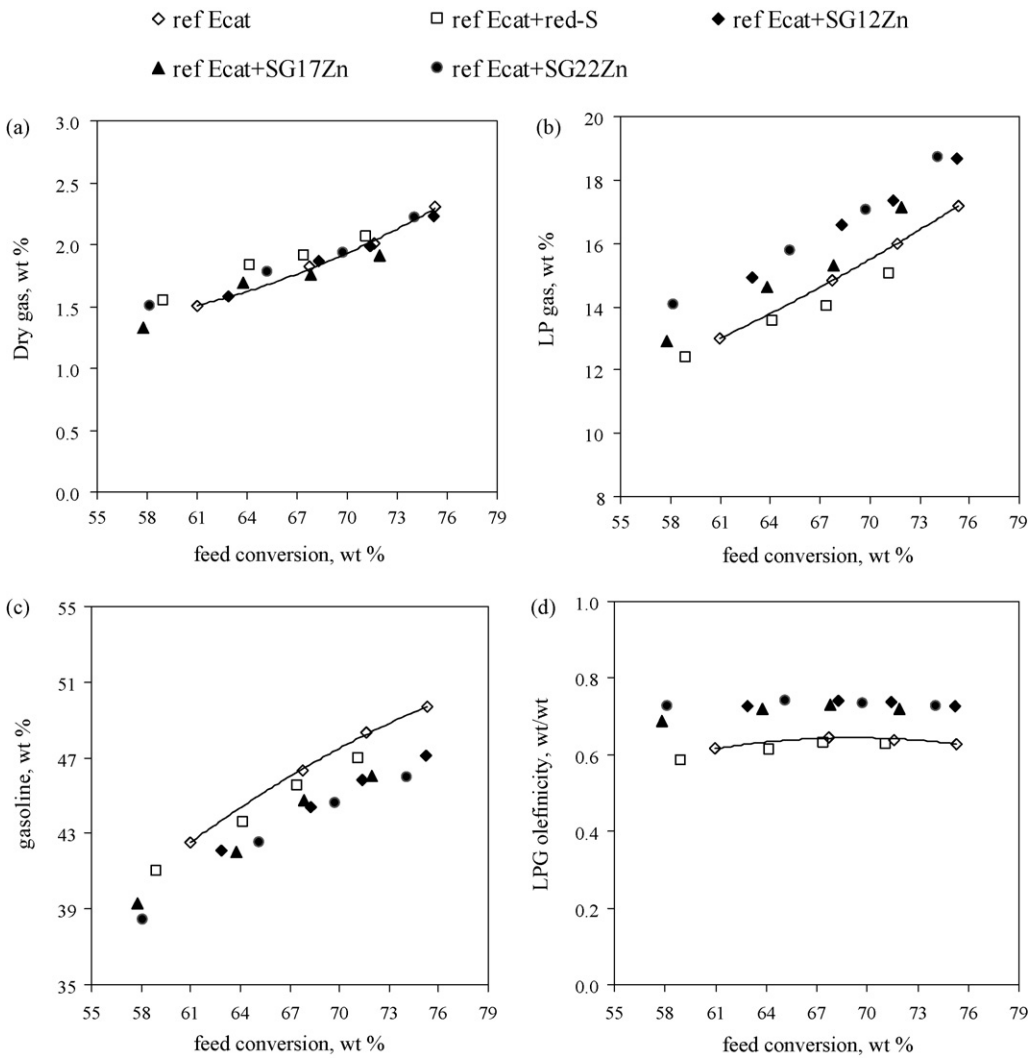

Fig. 4. Products distribution as a function of feed conversion: (a) dry gas yield, (b) LPG yield, (c) gasoline yield, and (d) LPG olefinicity. The solid line is a trend line drawn for the ref Ecat experimental cracking data.

a higher amount of coke being deposited on the catalyst because the amount of coke precursors in the feed to the mass of catalyst is higher. From this, Fig. 3 indicates that when working at a low C/O, corresponding to a relative high ratio fed coke precursors to catalyst amount, the trapping effect of the zinc-aluminates, in particular that of SG12Zn sample – the most acid one – is more evident. Assuming that part of the coke precursors are rapidly trapped on the zinc-aluminates, the Ecat is deactivated to a lesser extent and, hence, its cracking capacity increases reflecting in higher feed conversion.

3.2.2. Products distribution

The effect of the addition of the zinc-aluminates to the ref Ecat on the various cracking products, viz., dry gas, LPG, light olefins, gasoline, bottoms and coke, has been also investigated. It is desirable that the incorporation of the additives to the main catalyst does not modify significantly the base products distribution. In particular, the gasoline production should be kept while the dry gas and coke levels should not be significantly increased.

When comparing the products distribution of the ref Ecat/additive blends to the ref Ecat, some differences are detected for LPG, gasoline, coke and LPG olefinicity, as is illustrated in Figs. 4 and 5. On other hand, the yield of dry gas remains practically unchanged while the bottoms selectivity was just slightly modified, cfr. infra.

An increase in the LPG production was observed for the ref Ecat/additives blends compared with the ref Ecat. Such a higher LPG production may be originated by overcracking of hydrocarbons due to the substitution of zeolitic material of the ref Ecat in the reactor bed by additive.

Contrary to what was observed for LPG, gasoline yields decreased when zinc-aluminates were blended to the ref Ecat, as can be observed in Fig. 4. This indicates that gasoline, which is typically susceptible to secondary reactions, is in principle undergoing overcracking to produce LPG. The observed response of the gasoline fraction can be partially understood in terms of what occurs with the hydrogen transfer activity of the catalytic system. In brief, the fact of adding additives implies a dilution of the zeolitic portion of catalytic bed. It is

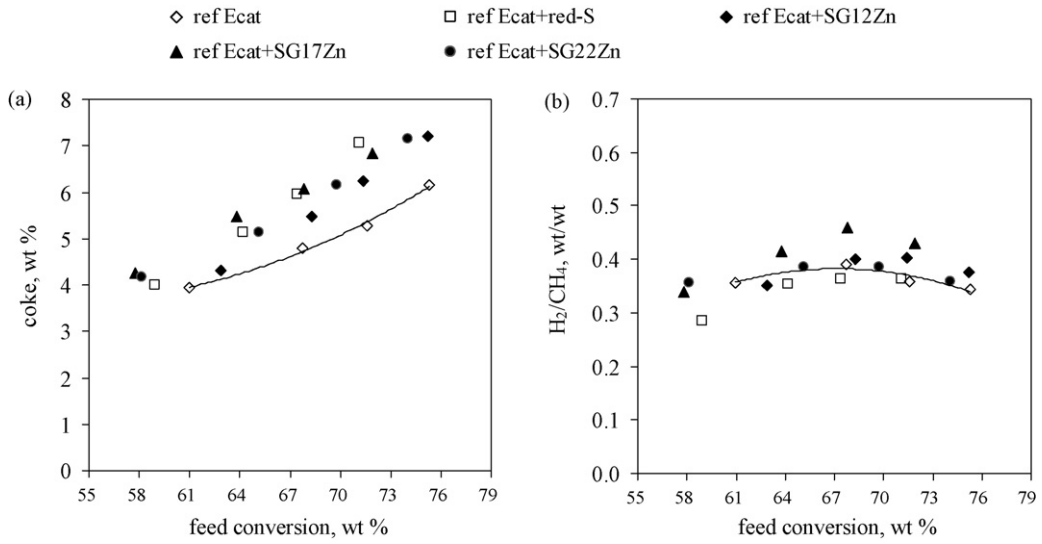

Fig. 5. Products distribution as a function of feed conversion: (a) coke yield and (b) H_2/CH_4 ratio. The solid line is a trend line drawn for the ref Ecat experimental cracking data.

known that the Brönsted sites in the zeolite are responsible of hydrogen transfer in cracking catalysts [34]. Secondary cracking and hydrogen transfer are in competition when a carbenium ion is adsorbed on the zeolite surface. The former reaction leads to the formation of a smaller carbenium ion and a gas phase species while the latter yields a saturated gas phase species. For the particular case of gasoline, lowering the number of acid sites responsible of transfer hydrogen reactions increases the possibilities of overcracking.

The observed increase in the olefins content in the LPG in Fig. 4 is another indication of a decrease in the relative participation of hydrogen transfer reactions for the ref Ecat/additive compared to the ref Ecat. Recall that olefins and naphthenes are consumed by a sequence of hydrogen transfer reactions and deprotonation reactions for producing paraffins and aromatics. Notice that the increase in the LPG olefinicity occurs to a similar extent for all the ref Ecat/zinc-aluminate blends, which seems to be attributed to a pure dilution effect of the main catalyst. Based on this and assuming that the increase in the LPG yield at expenses of the gasoline one is not dramatic, hydrogen transfer appears to be the most important cause, but not the only one, of this effect. A possible increase in the dehydrogenation rate due to the presence of the zinc-aluminates is, however, not appreciated in the olefinicity of the LPG.

Compared with ref Ecat, the incorporation of the zinc-aluminates and the reference additive to the reactor bed resulted in a small albeit appreciable increase in coke production. This in principle appears to be caused by a relative increase in the coking rates caused by the replacement of a zeolitic fraction in the reactor bed by additives as is displayed in Fig. 5a. In other words, zinc-aluminates are adsorbing selectively (poly)aromatic species which in turn are typical coke precursors due to their basic character.

Apart from the adsorption effect due to the Lewis acidity of the zinc-aluminates, an increase in the dehydrogenation rate by the presence of the zinc-aluminates is also promoting the formation of coke. It is widely accepted that dehydrogenation and hydride transfer reactions have a positive effect in coking [35]. By assuming that the decrease in the rate of hydride transfer rates is the same when using any of the additives by a dilution effect of the zeolitic portion of the ref Ecat in the reactor bed, the coking results suggests that the relative importance of dehydrogenation to hydrogen transfer increases in the presence of the zinc-aluminates. The dehydrogenating capacity of a FCC catalyst in qualitative terms is typically measured by means of the hydrogen to methane ratio. Fig. 5b shows that the addition of zinc-aluminates to the ref Ecat leads to an increase in the H_2/CH_4 with respect to the ref Ecat alone.

3.2.3. Gasoline composition

A detailed analysis of hydrocarbons (DHA) of cracked gasoline was performed to investigate a possible effect of the addition of the zinc-aluminates to the reactor bed on the gasoline composition and quality. This can provide additional information on the relative importance of the hydrogen transfer to the dehydrogenation reactions owing to the use of the zinc-aluminates.

Table 5 shows the DHA for the cracked gasoline from the various ref Ecat/additive blends compared with ref Ecat at a constant feed conversion equal to 70 wt%. Notice that the information in this table is given in terms of the mass of the hydrocarbon family formed to the mass of feed, in other words, the yield of the various hydrocarbon families constituting the gasoline.

At the used operating conditions, the hydrocarbons content of the cracked gasoline decreased in the following order: aromatics > paraffins > olefins > naphthenes. The composition of the gasoline produced with the ref Ecat/zinc-aluminate blends is not strictly the same than that from ref Ecat, based on the information in Table 5. A lower amount of aromatics, paraffins and naphthenes, and a higher proportion of olefins are observed for the ref Ecat/zinc-aluminate blends. This is

Table 5
Detailed hydrocarbon analysis, in terms of the mass of hydrocarbon family in the gasoline per mass of feed, and corresponding chromatographic octane number out of the cracking of the feed with properties displayed in Table 2 on the ref Ecat and the ref Ecat/additive blends at a constant feed conversion equal to 70 wt%

Sample	Paraffins	Aromatics	Naphthenes	Olefins	$\frac{RON+MON}{2}$
ref Ecat + SG12Zn	11.7	14.2	3.1	6.3	81.3
ref Ecat + SG17Zn	11.6	11.7	2.5	7.8	81.9
ref Ecat + SG22Zn	9.2	10.6	1.7	9.0	85.4
ref Ecat + red-S	13.5	13.7	3.0	6.7	81.7
ref Ecat	14.0	14.1	3.1	7.0	81.6

particularly true when adding the SG22Zn sample. The global decrease in the content of paraffins and aromatics and the increase of olefins match with the hypothesis of a decrease in the hydrogen transfer rate due to the replacement of base catalyst with zinc-aluminates. A promotion of the dehydrogenation rate in the presence of zinc-aluminates can also contribute to the observed increase in the olefins content. It is likely that the effect of the latter reaction on the aromatics is hidden by a selective adsorption of some aromatics on the Lewis sites of the zinc-aluminates which ultimately end up in coke, as was proposed in a previous section.

Despite the observed decrease in the aromatics content in the gasoline, a promotion of the GC-octane by almost 4 units for the SG22Zn sample is observed in Table 5. This sample, as will be pointed out below, is the one leading to the highest gasoline sulfur reduction levels. This octane increase is associated to the conservation of C_5-olefins which in turn report high values of blend octane.

3.3. Sulfur distribution in cracked products

3.3.1. Sulfur feed conversion

Analogously to what occurs on the hydrocarbons, the sulfur contained in the feed is distributed to the different products, i.e., gasoline, gases and coke, after cracking. An unconverted sulfur fraction remains in the LCO and HCO cuts. According to literature [36], after cracking the highest

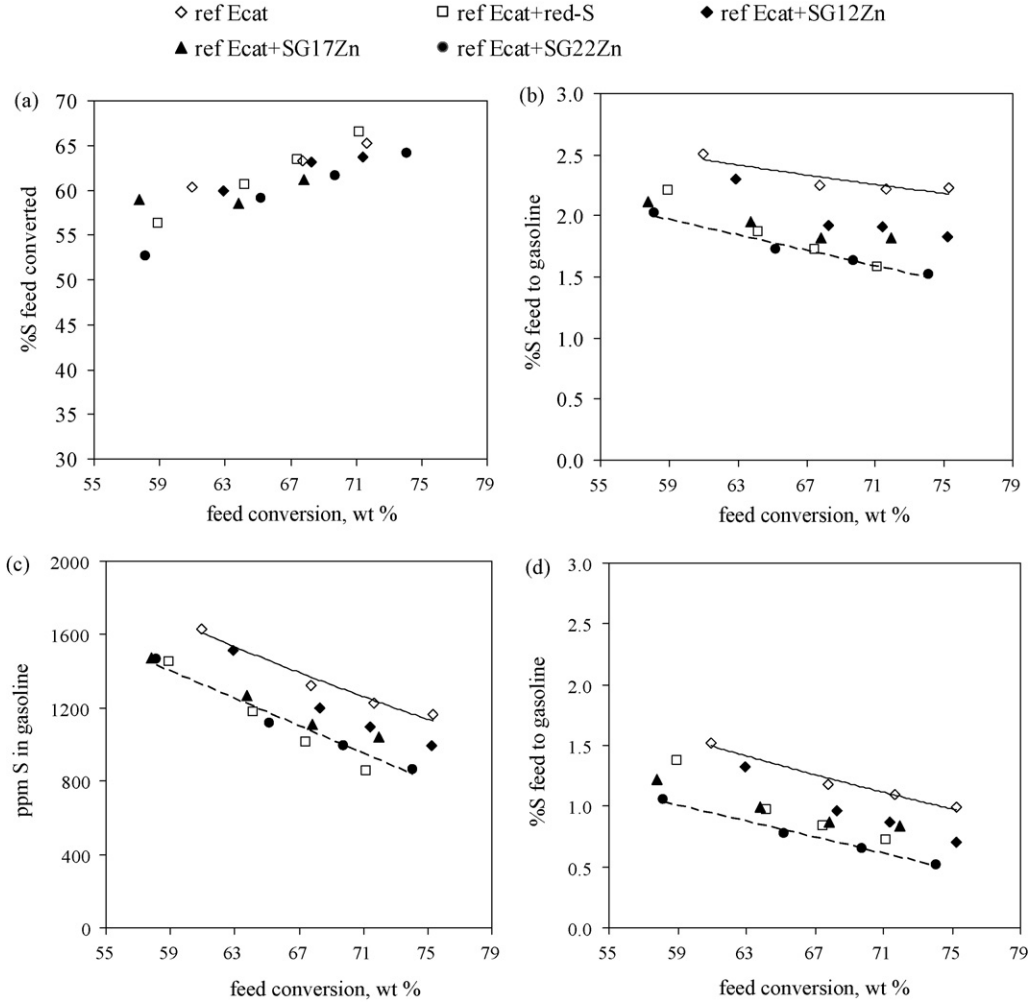

Fig. 6. (a) Sulfur feed converted as a function of feed conversion, (b) sulfur feed ending up in gasoline, including benzothiophene, as a function of feed conversion, (c) sulfur feed ending up in gasoline, excluding benzothiophene, as a function of feed conversion, and (d) sulfur concentration, including benzothiophene, in the cracked gasoline as a function of feed conversion. The trend lines in the figure are used for highlighting the differences between the ref Ecat response, solid line, and the ref Ecat/SG22Zn blend, dashed line.

proportion of the sulfur feed converted, i.e., up to 50 wt%, ends up in the dry gas as hydrogen sulfide. Only from 2 to 10 wt% and 3 to 20 wt% of the sulfur feed ends up in the gasoline and coke, respectively. Such percentages are strongly influenced by the catalyst formulation and, in particular, by the feed properties [13].

The sulfur feed conversion as a function of feed conversion is displayed in Fig. 6. It moderately increases with feed conversion independently of the ref Ecat/additive blend used and, at the operating conditions studied, it ranged from 50 to 70 wt%. Also from Fig. 6, one can see that there is no significant enhancement of the sulfur feed conversion with the addition of the additives. The susceptibility of the sulfur in the feed to cracking does not appears to be a strong function of the ref Ecat/additive blend used, in particular, at relatively high feed conversion. In literature the conversion of the sulfur species in the feed is more a function of the feed properties than of the catalyst (additive) ones [7,13].

3.3.2. Sulfur feed to gasoline

At the operation conditions investigated, the sulfur content in the produced cracked gasoline ranged from 850 to 1800 ppm as can be observed in Fig. 6. C_1 to C_4-alkylthiophenes and benzothiophene were, by far, the most prominent sulfur species in the cracked gasoline; the contribution of the former was higher than 50 wt% at relatively low feed conversion. A minor amount of thiols and tetrahydrothiophene were also detected. The concentration of all the so-called thiophenic species in gasoline but benzothiophene decreased with feed conversion showing that they are susceptible of secondary reactions, e.g., protonation, hydride transfer, dealkylation, disproportionation, cyclisation and isomerization.

Although the presence of the zinc-aluminates did not lead to an enhancement in the conversion of the sulfur feed, it had an effect on the sulfur feed incorporated to gasoline fraction with respect to that displayed by the ref Ecat, according to Fig. 6. In principle, this is an indication of a change in the kinetics of the cracking of the sulfur compounds.

According to Fig. 6, all the ref Ecat/zinc-aluminate blends exhibited a lower amount of the sulfur feed ended up in the gasoline fraction and, hence, a lower gasoline sulfur concentration compared with the ref Ecat. The sulfur reduction performance of the ref Ecat/additive blends can be more easily assessed using the information displayed in Table 6 that corresponds to data interpolated at 70 wt% of feed conversion. It is clear that the sulfur reduction in the gasoline increases with the zinc ($ZnAl_2O_4$) content in the zinc-aluminates. At 70 wt% of feed conversion, for instance, a sulfur reduction of 14, 19 and 35 wt%, based on the sulfur feed ended up in the gasoline cut including benzothiophene was observed with the samples SG12Zn, SG17 and SG22Zn, respectively. The gasoline sulfur reduction level for the sample SG22Zn is even higher than that displayed by the commercial additive red-S. The sulfur reduction level further increases to about 50% for the SG22Zn sample when benzothiophene is excluded from the gasoline cut, as is presented in Fig. 6b and c.

The observed decrease in the sulfur content in the gasoline is mainly caused by a decrease in the concentration of C_1 to C_4-alkylthiophenes and, to a lesser extent, thiophene, despite the fact that the relative decrease in the concentration of the latter is significant as can be observed in Fig. 7 and Table 6. Within alkylthiophenes, the highest sulfur reduction occurs on C_1 and C_2-alkylthiophenes while the lowest does on C_4-alkylthiophenes. The low reactivity of the remaining C_4-alkylthiophenes in the gasoline fraction indicates that they are highly branched and, thus, rather stable species. The amount of benzothiophene, on the other hand, is slightly affected by the presence of some additives. These results are qualitatively in agreement to what has been reported by others [13,16,19].

The effect of the additive to remove sulfur from the cracked gasoline should be strictly related to the kinetics of the cracked gasoline sulfur compounds already formed along with the kinetics of sulfur feed compounds that are, indeed, precursors of the cracked gasoline sulfur species. Recall that the sulfur compounds in the feed, many of them having an aromatic character, can enter to a cracking or to a coking pathway [6,37].

Focused on the kinetics of the gasoline sulfur compounds, explanations for the sulfur reduction have been formulated in terms of an increase of the hydrogen transfer reactions in the case of catalysts [2,14,38], whereas in the case of additives it

Table 6
Summary of the performance of the ref Ecat and the ref Ecat/additive blends in terms of the sulfur feed converted to gasoline (sulfur species), ppm of sulfur in gasoline and gasoline sulfur reduction, corresponding to data interpolated at 70 wt% of feed conversion

	ref Ecat + SG12Zn	ref Ecat + SG17Zn	ref Ecat + SG22Zn	ref Ecat + red-S	ref Ecat
ppm sulfur in gasoline	1153	1078	868	966	1283
Percentage sulfur feed to gasoline	1.92	1.82	1.46	1.68	2.24
Percentage sulfur feed to species in gasoline					
Thiophene	0.07	0.06	0.02	0.06	0.10
C_1-alkylthiophenes	0.21	0.20	0.12	0.17	0.30
C_2-alkylthiophenes	0.24	0.23	0.16	0.20	0.33
C_3-alkylthiophenes	0.18	0.17	0.13	0.17	0.22
C_4-alkylthiophenes	0.11	0.11	0.08	0.11	0.13
Benzothiophene	1.00	0.97	0.98	0.88	1.09
Percentage gasoline sulfur reduction[a]	14.3	18.8	34.8	25.0	–

[a] Calculated based on the percentage sulfur feed in gasoline and with respect to the ref Ecat.

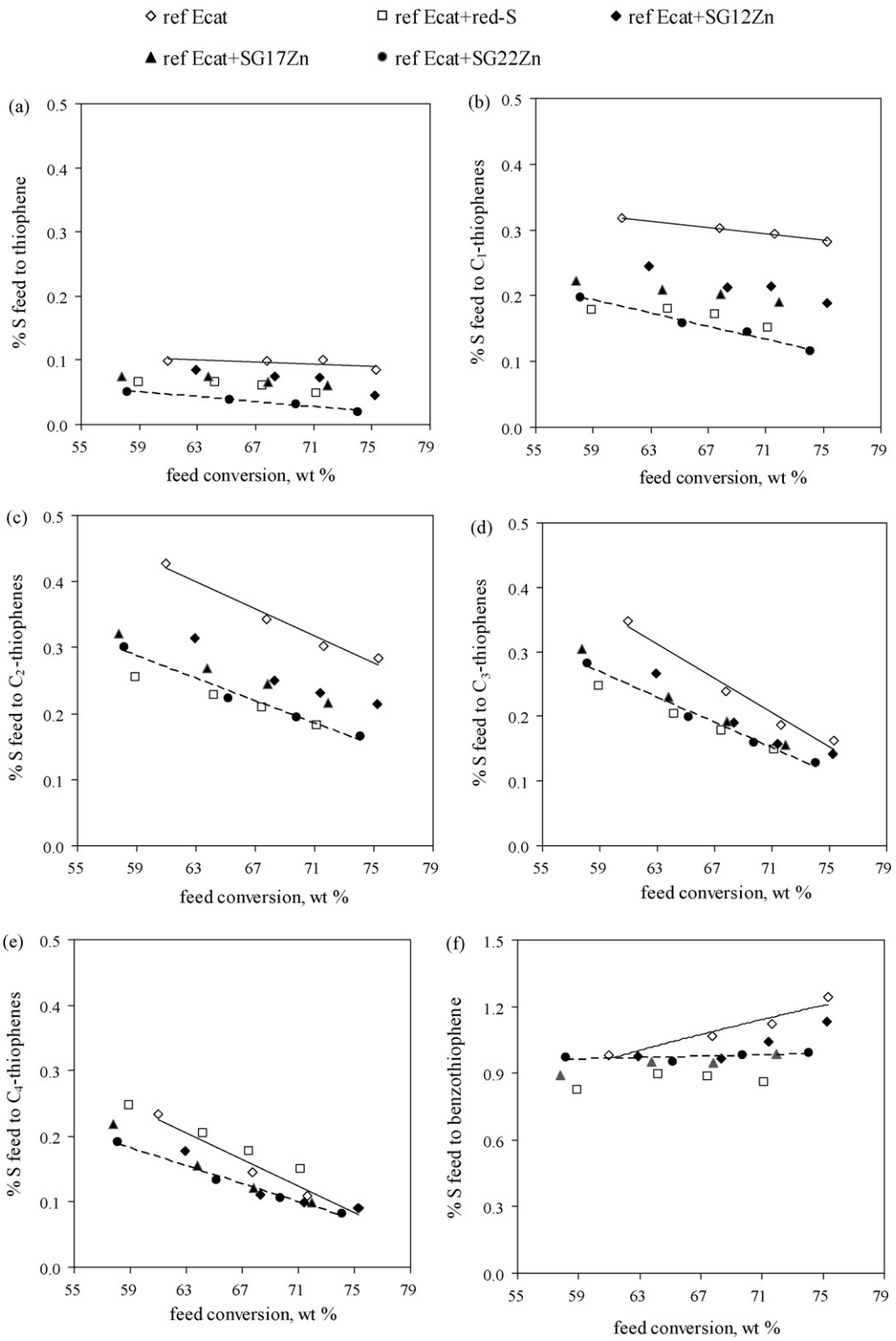

Fig. 7. Percentage of the sulfur feed converted to (a) thiophene, (b) C_1-alkylthiophenes, (c) C_2-alkylthiophenes, (d) C_3-alkylthiophenes, (e) C_4-alkylthiophenes and (f) benzothiophene, as a function of feed conversion. The trend lines in the figure are used for highlighting the differences between the ref Ecat response, solid line, and the ref Ecat/SG22Zn blend, dashed line.

has been associated to a preferential adsorption of sulfur compounds on Lewis acid sites [13,19].

In our study, there are evidences that Lewis acid sites are playing a role on the sulfur reduction owing to the higher acidity of the zinc-aluminates with respect to the ref Ecat, as is reported in Table 4. But the fact that zinc-aluminates with a higher Lewis acidity did not exhibit a better gasoline sulfur reduction capacity is, in principle, in disagreement with what is

commonly reported in literature [18,19]. In a recent publication [21], however, a fluoride doped γ-alumina with a higher Lewis acidity compared with a zinc doped γ-alumina displayed a lower gasoline sulfur reduction capacity. Anderson et al. [16] also found within a series of additives containing Zn and Mn on alumina and titania, that the one with the lowest amount of Lewis acid sites exhibited the best results in terms of gasoline sulfur reduction. These facts suggest that a higher Lewis acidity does not yield unfailingly higher sulfur reduction. According to what was discussed in a previous section, it appears that there are active sites for gasoline sulfur reduction associated to the $ZnAl_2O_4$ spinel formed. The good capacity of $ZnAl_2O_4$ contained in the zinc-aluminates to adsorb aromatic-like compounds, thiophenes among them, was demonstrated in a previous section with the decrease in the aromatics content in the gasoline showed by the ref Ecat/SG22Zn blend. Once adsorbed, thiophenic compounds can undergo cracking without a previous saturation [39] or can be saturated to produce tetrahydrothiophenes that are further cracked [14,21]. The former possibility is, however, energetically very demanding [40].

Based on this and on our own results, it is also reasonable to assume that hydrogen generated in situ on the additive may play a role in a further gasoline sulfur reduction by a saturation of thiophenic compounds adsorbed on the additive. The formed saturated thiophenic species are more susceptible to cracking compared with saturated ones. The former are ultimately converted to olefins and H_2S via an acid mechanism on Brönsted sites through a set of hydride transfer, ring-opening, (de)protonation, isomerization and β-scission reactions.

4. Conclusions

The addition of zinc-aluminates, prepared by sol–gel, to a commercial equilibrium catalyst leads to a sulfur reduction of up to 35 wt%, considering benzothiophene, and of up to 50% excluding benzothiophene, which is comparable with reduction levels reported by commercial additives. The gasoline sulfur reduction is basically the result of a decrease in the amount of C_1–C_4-alkylthiophenes and, to a lesser extent, thiophene. The zinc ($ZnAl_2O_4$) content is found to increase the sulfur reduction capacity of the zinc-aluminates.

At the cracking conditions used, adding zinc-aluminates to the reactor bed modifies moderately feed conversion and the products distribution, in particular, a decrease in the gasoline production, an increase in coking and an enhancement in the gasoline quality. It is proposed that besides the direct cracking of adsorbed thiophenic species on the additive, a further gasoline sulfur decrease can occur via cracking of saturated thiophenic species formed via hydrogenation of adsorbed thiophenic species with hydrogen produced in situ in the additive. The reported results also demonstrate that additives with higher Lewis acidity are not necessarily more effective reducing the sulfur in cracked gasoline.

Acknowledgement

Funding from the Maya Crude Oil Processing Research Program, Project D.01024, as a part of a scientific collaboration program between the IMP and PEMEX-Refinacion.

References

[1] G. Wang, J.S. Gao, Ch.M. Xu, Pet. Sci. Technol. 11–12 (2004) 1581.
[2] R.H. Harding, X. Zhao, K. Qian, K. Rajagopalan, W.C. Cheng, Ind. Eng. Chem. Res. 35 (1996) 2561.
[3] L.L. Upson, W. Schainth, Oil Gas J. 95 (49) (1997) 47.
[4] H. Ming-Yuan, Catal. Today 73 (2002) 49.
[5] I.V. Babich, J.A. Moulijn, Fuel 82 (2003) 607.
[6] F.J. Hernández-Beltrán, J.C. Moreno-Mayorga, R. Quintana-Solórzano, J. Sánchez-Valente, F. Pedraza-Archila, M. Pérez-Luna, Appl. Catal. B: Environ. 34 (2001) 137.
[7] J.A. Valla, A.A. Lappas, I.A. Vasalos, C.W. Kuehler, N.J. Gudde, Appl. Catal. A 276 (2004) 75.
[8] T.G. Kaufmanna, A. Kaldor, G.F. Stuntz, M.C. Kerby, L.L. Ansell, Catal. Today 62 (2000) 77.
[9] S. Brunet, D. Mey, G. Perot, C. Bouchy, F. Diehl, Appl. Catal. A 278 (2005) 143.
[10] W.C. Cheng, G. Kim, A.W. Peters, X. Zhao, K. Rajagopalan, Catal. Rev. Sci. Eng. 40 (1–2) (1998) 39.
[11] F. Baco, J.J. Beboulene, S. Carbonneaux, J.P. Durang, N. Marchal-Georges, F. Picard, E. Roche, 12th Saudi-Japanese Symposium on Catalysis in Petroleum Refining and Petrochemicals, KFUPM-Research Institute, Dhahran, Saudi Arabia, 2002.
[12] M.A.B. Siddiqui, A.M. Aitani, Pet. Sci. Technol. 25 (3–4) (2007) 299.
[13] F.J. Hernández-Beltrán, R. Quintana-Solórzano, J. Sánchez-Valente, F. Pedraza-Archila, F. Figueras, Appl. Catal. B: Environ. 42 (2003) 145.
[14] A. Corma, C. Martínez, G. Ketley, G. Blair, Appl. Catal. A 208 (2001) 135.
[15] P. Leflaive, J.L. Lemberton, G. Perot, C. Mirgain, J.Y. Carriat, J.M. Colin, Appl. Catal. A: Gen. 227 (2002) 201.
[16] P-O.F. Anderson, M. Pirjamali, S.G. Järas, M. Boutonnet-Kizling, Catal. Today 53 (1999) 565.
[17] M.A.B. Siddiqui, S. Ahmed, A.M. Aitani, C.F. Dean, Appl. Catal. A: Gen. 303 (2006) 116.
[18] A.A. Vargas-Tah, R. Cuevas-Garcia, L.F. Pedraza-Archila, J. Ramirez-Solís, A.J. García-López, Catal. Today 107–108 (2005) 713.
[19] X. Zhao, W.-C. Cheng, J.A. Rudesill, R.F. Wormsbecher, P.S. Deitz, US Patent 6,635,168, W.R. Grace & Co.-Conn, 2003.
[20] C.F. Dean, A.M. Aitani, M.R. Sabed, M.A.B. Siddiqui, Pet. Sci. Technol. 21 (7–8) (2003) 1265.
[21] F. Can, A. Travert, V. Raux, J.P. Glison, F. Mauge, R. Hu, R.F. Wormsbecher, J. Catal. 249 (2007) 79.
[22] R. Sadeghbeigi, Fluid Catalytic Cracking Handbook, second ed., Gulf Professional Publishing, USA, 2000.
[23] M.F. Reyniers, H. Beirnaert, G.B. Marin, Appl. Catal. A: Gen. 202 (2000) 49.
[24] R. Quintana-Solórzano, J.W. Thybaut, G.B. Marin, Appl. Catal. A: Gen. 314 (2006) 184.
[25] J. Sanchez-Valente, X. Bokhimi, F. Hernández, Langmuir 19 (2003) 3583.
[26] J. Sanchez-Valente, X. Bokhimi, J.A. Toledo, Appl. Catal. A: Gen. 264 (2004) 175.
[27] H. Grabowska, W. Mista, J. Trawczynski, J. Wrzyszcz, Appl. Catal. A: Gen. 220 (2001) 207.
[28] E.P. Parry, J. Catal. 2 (1963) 371.
[29] K. Arata, Adv. Catal. 37 (1990) 165.
[30] D. Coster, A.L. Blumenfeld, J.J. Fripiat, J. Phys. Chem. 98 (1994) 6201.
[31] R.W. Grimes, A.B. Anderson, A.H. Heuerg, J. Am. Chem. Soc. 111 (1989) 1.
[32] W.P. Hettinger, Catal. Today 53 (1999) 367.
[33] R. Wormsbecher, G. Kim, US Patent 5,376,608 (December 24, 1994).
[34] K.A. Cumming, B.W. Wojciechiwski, Catal. Rev. Sci. Eng. 38-1 (1996) 101.

[35] H.S. Cerqueira, P. Magnoux, D. Martin, M. Guisnet, Appl. Catal. A: Gen. 108 (2001) 359.
[36] E.G. Wollanston, W.L. Forsythe, I.A. Vasalos, Oil Gas J. 2 (1971) 64.
[37] X. Dupain, L.J. Rogier, E.D. Gamas, M. Makkee, J.A. Moulijn, Appl. Catal. A: Gen. 238 (2003) 223.
[38] T. Myrstad, B. Seljestokken, H. Ergan, E. Rytter, Appl. Catal. A: Gen. 192 (2000) 299.
[39] X. Saintigny, R.A. van Santen, S. Clemendot, F. Hutschka, J. Catal. 183 (1999) 107.
[40] J.A. Valla, A.A. Lappas, I.A. Vasalos, Appl. Catal. A: Gen. 297 (2006) 90.